

Convection Heat Transfer and Flow Calculations Suitable for Electric Machines Thermal Models

*Original*

Convection Heat Transfer and Flow Calculations Suitable for Electric Machines Thermal Models / D. A., Staton; Cavagnino, Andrea. - In: IEEE TRANSACTIONS ON INDUSTRIAL ELECTRONICS. - ISSN 0278-0046. - 55:10(2008), pp. 3509-3516. [10.1109/TIE.2008.922604]

*Availability:*

This version is available at: 11583/1849631 since:

*Publisher:*

IEEE

*Published*

DOI:10.1109/TIE.2008.922604

*Terms of use:*

This article is made available under terms and conditions as specified in the corresponding bibliographic description in the repository

*Publisher copyright*

(Article begins on next page)

# Convection Heat Transfer and Flow Calculations Suitable for Electric Machines Thermal Models

David A. Staton and Andrea Cavagnino, *Member, IEEE*

**Abstract**—This paper deals with the formulations used to predict convection cooling and flow in electric machines. Empirical dimensionless analysis formulations are used to calculate convection heat transfer. The particular formulation used is selected to match the geometry of the surface under consideration and the cooling type used. Flow network analysis, which is used to study the ventilation inside the machine, is also presented. In order to focus the discussion using examples, a commercial software package dedicated to motor cooling optimization (Motor-CAD) is considered. This paper provides guidelines for choosing suitable thermal and flow network formulations and setting any calibration parameters used. It may also be considered a reference paper that brings together useful heat transfer and flow formulations that can be successfully applied to thermal analysis of electrical machines.

**Index Terms**—Dimensionless correlations, electrical machines, flow analysis, thermal model.

## I. INTRODUCTION

OVER THE past decade, thermal analysis of electric machines has started to receive more attention. In fact, with the increasing requirements for miniaturization, energy efficiency, cost reduction, and the need to fully exploit new topologies and materials, it is now necessary to analyze the thermal circuit to the same extent as the electromagnetic design. An increase in the level and sophistication of thermal analysis used in the design process also gives benefits in terms of a faster time to market and a greater chance that the developed solution more closely matches the customer's requirements. During the same period, there has also been more interest in thermal analysis of drives and power converters [1], [2].

The lumped parameter thermal network (LPTN) method has been successfully used for thermal analysis of electric motors and [3] represents a notable example. This commercial software package provides near-instantaneous calculation speeds, allowing “what-if” scenarios to be run in real time. The users input geometric data for the design under consideration using the radial and cross-sectional graphical editors. Materials and the cooling system type to be used in the machine are then selected. All thermal parameters, such as conduction, radiation, and convection thermal resistances, are then calculated by the program, and the thermal performance is evaluated.

Manuscript received November 23, 2007; revised March 10, 2008. Current version published October 1, 2008.

D. A. Staton is with Motor Design Ltd., Shropshire SY12 OEG, U.K. (e-mail: dave.staton@motor-design.com).

A. Cavagnino is with the Electrical Machines Laboratory, Department of Electrical Engineering, Politecnico di Torino, 10129 Torino, Italy (e-mail: andrea.cavagnino@polito.it).

Color versions of one or more of the figures in this paper are available online at <http://ieeexplore.ieee.org>.

Digital Object Identifier 10.1109/TIE.2008.922604

The formulations for the thermal resistances are quite simple. The conduction resistance is equal to the path length divided by the product of the path area and the material's thermal conductivity. The convection and radiation resistances are equal to one divided by the product of the surface area and the heat transfer coefficient. The radiation heat transfer coefficient is simply a function of the surface properties, i.e., the emissivity and the view factor. The emissivity is known for different types of surface, and the view factor can be calculated based on the geometry. An experimental approach to the radiation phenomena that occurs both inside and outside the machine can be found in [4].

The convection heat transfer coefficient is most often calculated using empirical formulations based on convection correlations, which are readily available in the heat transfer literature [5]–[8]. Fortunately, there is a wealth of convection correlations for most of the basic geometric shapes used in electrical machines, both for natural and forced convection cooling i.e., cylindrical surfaces, flat plates, open fin channels, closed fin channels, etc. In this paper, the most common and useful dimensionless correlations used for calculating convection heat transfer in electrical machines are reported. Since forced convection heat transfer from a given surface depends on the fluid local velocity [9]–[14], flow network analysis is also presented. In this case, empirical dimensionless formulations are used to predict pressure drops due to flow restrictions, i.e., vents, bends, contractions, and expansions, and, ultimately, to calculate the airflow and resulting air velocity in all ventilation paths.

This paper aims at assisting non-heat transfer specialists in their understanding of heat transfer and flow analysis. It may also be considered a reference that brings together useful heat transfer and flow formulations that can be successfully applied to thermal analysis of electrical machines.

## II. CONVECTION DIMENSIONLESS ANALYSIS

Convection is the heat transfer process due to fluid motion. In natural convection, the fluid motion is due entirely to buoyancy forces arising from density variations in the fluid. In a forced convection system, the fluid movement is by an external force, e.g., fan, blower, and pump. If the fluid velocity is large, then turbulence is induced. In such cases, the mixing of hot and cold air is more efficient, and there is an increase in heat transfer. The turbulent flow will, however, result in a larger pressure drop such that with a given fan/pump, the fluid flow rate will be reduced.

Proven empirical heat transfer correlations based on dimensionless analysis are used to predict the heat transfer coefficient

$h$  [W/(m<sup>2</sup> °C)] for all convection surfaces in the machine [5]–[8], [15], [16]. Many such correlations are built in [3], where the most appropriate formulation for a given surface and flow condition is automatically chosen. This means that the user need not be an expert in heat transfer analysis to use the software effectively.

Forced convection heat transfer from a given surface is a function of the local flow velocity. In order to predict the local velocity, a flow network analysis can be used to calculate the flow of fluid (air or liquid) inside the machine. Empirical dimensionless analysis formulations are used to predict pressure drops for flow restrictions such as vents, bends, contractions, and expansions.

For natural convection, the typical form of the convection correlation is shown as follows:

$$Nu = a \cdot (Gr \cdot Pr)^b \tag{1}$$

For forced convection, the typical form of the convection correlation is

$$Nu = a \cdot (Re)^b \cdot (Pr)^c \tag{2}$$

where  $a$ ,  $b$ , and  $c$  are constants given in the correlation. The following correlations also have to be considered:

$$Re = \rho \cdot v \cdot L / \mu \tag{3}$$

$$Gr = \beta \cdot g \cdot \Delta T \cdot \rho^2 \cdot L^3 / \mu^2 \tag{4}$$

$$Pr = c_p \cdot \mu / k \tag{5}$$

$$Nu = h \cdot L / k \tag{6}$$

where

- Nu Nusselt number;
- Re Reynolds number;
- Gr Grashof number;
- Pr Prandtl number;
- $h$  heat transfer coefficient [W/(m<sup>2</sup> °C)];
- $\mu$  fluid dynamic viscosity (in kilograms per second meter);
- $\rho$  fluid density (in kilograms per cubic meter);
- $k$  fluid thermal conductivity [W/(m °C)];
- $c_p$  fluid specific heat capacity [kJ/(kg °C)];
- $v$  fluid velocity (in meters per second);
- $\Delta T$  difference between surface and fluid temperatures (in degrees Celsius);
- $L$  characteristic length of the surface (in meters);
- $\beta$  coefficient of cubical expansion [1/K]; for the gases,  $\beta = 1/(273 + T_{FLUID})$
- $g$  gravitational attraction force (in meters per second squared).

The magnitude of  $Re$  is used to judge if there is laminar or turbulent flow in a forced convection system. Similarly, the  $Gr \cdot Pr$  product is used in natural convection systems.

The most important parameter to be considered is  $h$ . Once  $h$  is known, it is possible to calculate the thermal resistance to put

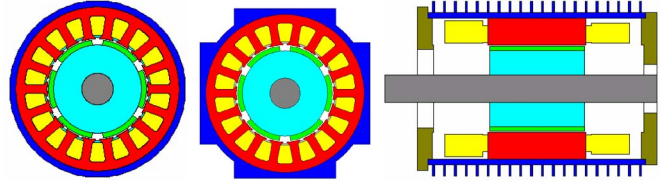


Fig. 1. Examples of housing types that are suitable for a TENV cooling system.

in the heat transfer network by the following equation, where  $A$  [m<sup>2</sup>] is the surface area

$$R = 1 / (h \cdot A) \tag{7}$$

Natural convection heat transfer is a primary function of the fluid properties and of the temperature difference between the considered solid component and the fluid. Forced convection is a primary function of the fluid velocity and fluid properties, and it is a secondary function of the temperature because the fluid properties are temperature dependent.

The advantage of using empirical formulations based on dimensionless analysis is that the same formulation can be used for similarly shaped geometries with a size that is different from that of the original experiments and/or with a different fluid. In addition, altitude has a significant effect on convection cooling and is fully accounted for, as the variation in air pressure, density, and temperature variation with altitude can easily be modeled.

The mixed heat transfer due to the combination of natural and forced convection is estimated using

$$h_{Mixed}^3 = h_{Forced}^3 \pm h_{Natural}^3 \tag{8}$$

The fluid flux direction determines the sign that has to be used in (8): a + sign for assisting and transverse flow and a – sign for opposing types of flow [5].

### III. NATURAL CONVECTION: TENV COOLING SYSTEM

In a total enclosed nonventilated (TENV) electric machine, the external surface of the housing dissipates heat by natural convection and radiation. A few examples of housing types that are designed for TENV cooling are shown in Fig. 1. In such a cooling system, the outer surface is usually smooth. If fins are used to increase the convection surface, they should be oriented so as not to disturb the natural airflow, as shown in the radial fin design in the motor on the right part of Fig. 1, where the fins are perpendicular to the machine shaft, so the convection cooling is only optimal if the motor is mounted horizontally in the application. If a radial finned housing is used in an application with a vertical mounting, then some derating must be applied. This situation is depicted in Fig. 2.

The calculation of natural convection heat transfer is often a requirement for axial finned housing used in fan-cooled machines, as shown in Fig. 4. This is because natural convection can dominate the cooling at low fan speeds, as in the case of motors used in variable-speed drives.

Correlations for basic shapes such as horizontal and vertical cylinders and flat plates can be used to predict the convection

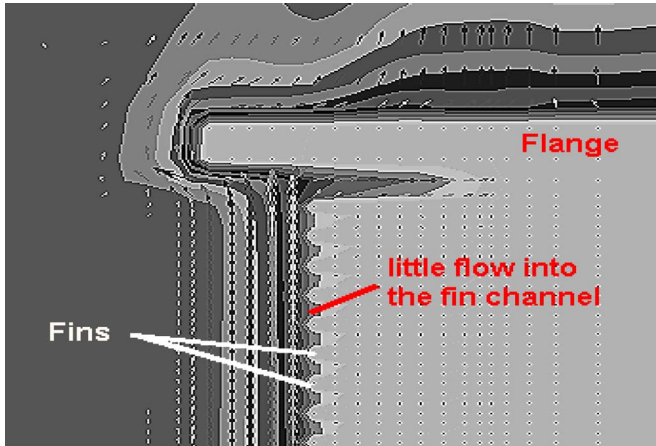


Fig. 2. Computational fluid dynamics (CFD) analysis results—radial fins with vertical shaft mounting.

TABLE I  
NATURAL CONVECTION CORRELATION COEFFICIENTS

| Shape                | $Gr \cdot Pr$<br>lam to turb | a<br>lam. | b<br>lam. | a<br>turb. | b<br>turb. |
|----------------------|------------------------------|-----------|-----------|------------|------------|
| Horizontal cylinder  | $10^9$                       | 0.525     | 0.25      | 0.129      | 0.33       |
| Vertical cylinder    | $10^9$                       | 0.59      | 0.25      | 0.129      | 0.33       |
| Vertical flat plate  | $10^9$                       | 0.59      | 0.25      | 0.129      | 0.33       |
| Horiz. plate [upper] | $10^8$                       | 0.54      | 0.25      | 0.14       | 0.33       |
| Horiz. plate [lower] | $10^5$                       | 0.25      | 0.25      | NA         | NA         |

heat transfer for the more simple smooth housing structures found in electrical machines. Table I gives suitable values for  $a$  and  $b$  coefficients to be used in (1) for such housing surfaces. Values are given for both laminar and turbulent flow, together with the  $Gr \cdot Pr$  product at which the transition to turbulent flow occurs [5]–[7].

For more complex housing types with finned structures, correlations for horizontal and vertical U-shaped channels are required.

For U-shaped vertical channels with laminar flow, (9), shown at the bottom of the page, can be used [16], where  $S$  is the fin spacing,  $L$  is the fin depth,  $\alpha = S/L$  is the channel aspect ratio, and  $r$  is the characteristic length (hydraulic radius) equal to  $2 \cdot L \cdot S / [2 \cdot (L + S)]$  for the case under study.

For a U-shaped horizontal channel with laminar flow [17], the following equation can be used:

$$Nu = 0.00067 \cdot Gr \cdot Pr \cdot \left\{ 1 - e^{(-7640/Gr \cdot Pr)^{0.44}} \right\}^{1.7}. \quad (10)$$

In this case, the fin spacing is used as the characteristic length.

The convection correlation chosen for a particular housing section depends on its geometry and orientation. Many corre-

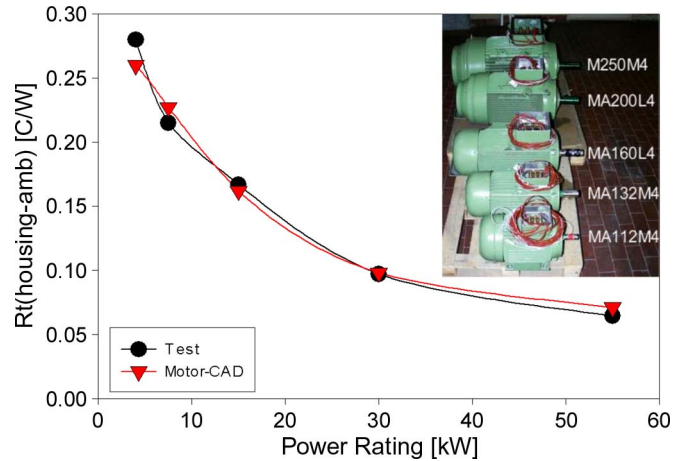


Fig. 3. Comparison between the measured and calculated housing to ambient natural convection thermal resistance for five four-pole 50-Hz 400-V TEFC induction motors rated 4, 7.5, 15, 30, and 55 kW.

lation types are required to suit the varied housing geometries used in practice. In many cases, the housing shape may be so complex that a single correlation does not exist. In such cases, separate correlations are used for the parts of the surface that have a shape with a known correlation. An area-based average is then carried out using the different correlations. For example, the following basic geometric shapes can be seen in a horizontally mounted radial finned motor housing (rightmost motor in Fig. 1): a cylinder for the main body of the housing; vertical fin channels on the two sides of the machine; and horizontal fin channels on the top and bottom of the machine. However, when the same machine is mounted with a vertical shaft orientation, as shown in Fig. 2, a more complex formulation has to be used. In this case, there is little air circulation at the base of deep narrow fin channels fitted to the sides of the motor. For such fin structures, terms are introduced into the formulation to limit the dissipation area to a depth down the fin channel equal to fin spacing. This is required so that the dissipation from such finned housings with a suboptimal orientation is not overpredicted. Indeed, good results can be obtained for such housing types [18].

Fig. 3 proves that a good prediction of the natural convection can be achieved by using such complex correlations. The machines have axial fins, rather than the radial fins considered in the previous example. Natural convection is suboptimal in this case, as the shaft is horizontal; so the fin channels are perpendicular to the natural airflow. Fig. 3 shows close agreement between the calculated and measured housing to ambient thermal resistance for the motors shown in the diagram, with the fan being at rest in this case [9].

$$Nu = \frac{r}{L} \cdot \frac{Gr \cdot Pr}{Z} \cdot \left[ 1 - e^{-Z \cdot \left( \frac{0.5}{(r/L) \cdot Gr \cdot Pr} \right)^{0.75}} \right]$$

$$Z = 24 \cdot \frac{1 - 0.483 \cdot e^{-0.17/\alpha}}{\left\{ [1 + \alpha/2] \cdot \left\{ 1 + (1 - e^{-0.83 \cdot \alpha}) \cdot (9.14 \cdot \sqrt{\alpha} \cdot e^{-465 \cdot S} - 0.61) \right\} \right\}^3} \quad (9)$$

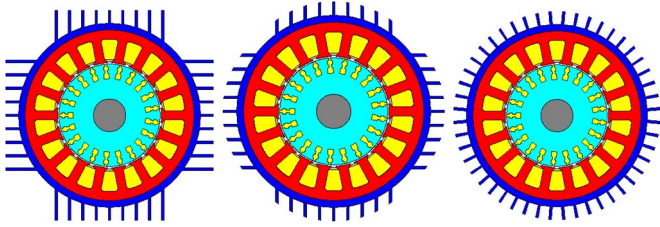


Fig. 4. Examples of housing types that are suitable for a TEFC cooling system.

IV. FORCED CONVECTION: TEFC COOLING SYSTEM

In a total enclosed fan-cooled (TEFC) electric machine, forced convection heat transfer gives improved dissipation, compared to an equivalent TENV machine. Some examples of the housing types optimized for external forced convection are shown in Fig. 4. A fan is usually fitted to the end of the shaft; the fan blows air in an axial direction over the outside of the housing. If the surface is smooth, it is possible to use the following well-known correlations, which are valid for flow over a flat plate [5]–[7]:

$$\text{Laminar flow (Re} < 5 \times 10^5 \text{) and (0.6} < \text{Pr} < 50 \text{)}$$

$$\text{Nu} = 0.664 \cdot \text{Re}^{0.5} \cdot \text{Pr}^{0.33} \tag{11}$$

$$\text{Turbulent flow (Re} > 5 \times 10^5 \text{)}$$

$$\text{Nu} = (0.037 \cdot \text{Re}^{0.8} - 871) \cdot \text{Pr}^{0.33} \tag{12}$$

The flat plate correlation can be used for a cylindrical housing when the airflow is along its axial length, as the surface is flat for each filament of air. In the TEFC machine, axial fins are usually included on the housing surface to increase the convection heat transfer. Furthermore, in the majority of TEFC machines, the fin channels are semiopen, and the most common external and internal flow correlations are not directly applicable. A special formulation for semiopen channels can be used. This is based on the extensive testing carried out by Heiles on finned induction motor housings of various sizes and shapes [15]. In the correlation, it is assumed that the flow is always turbulent due to the fact that the radial fans and cowlings used in such machines create turbulence. The convection heat transfer coefficient  $h$  is calculated using

$$h = \frac{\rho \cdot c_p \cdot D \cdot v}{4 \cdot L} \cdot (1 - e^{-m}) \tag{13}$$

$$m = 0.1448 \cdot \frac{L^{0.946}}{D^{1.16}} \cdot \left( \frac{k}{\rho \cdot c_p \cdot v} \right)^{0.214} \tag{14}$$

where  $v$  is the inlet air velocity in the fin channels,  $D$  is the hydraulic diameter (four times the channel area divided by the channel perimeter, including the open side), and  $L$  is the axial length of cooling fins. Heiles recommends that  $h$  is multiplied by a turbulence factor. The experimental tests indicated typical turbulence factor values in the range of 1.7–1.9, and this is independent of the flow velocity.

The inlet air velocity  $v$  has to be estimated. It is possible to use experimental data, such as those shown in Fig. 5, which are valid for four-pole 50-Hz machines. This shows the average air velocity at the start of the fin channels (fan side) for five TEFC induction motors. As expected, the air velocity versus

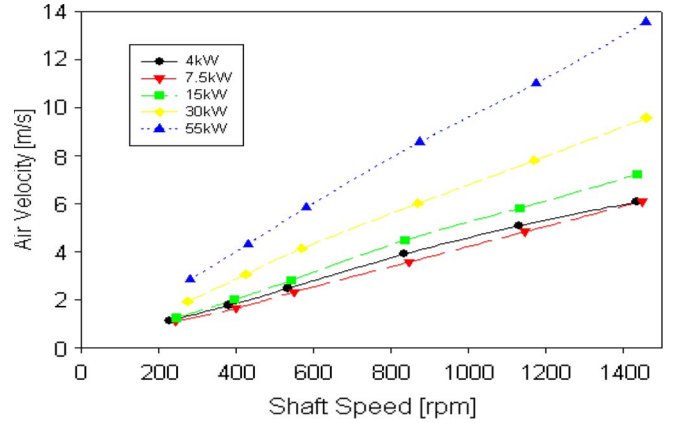


Fig. 5. Fin channel inlet air velocity versus the rotor speed for the TEFC induction motors shown in Fig. 3.

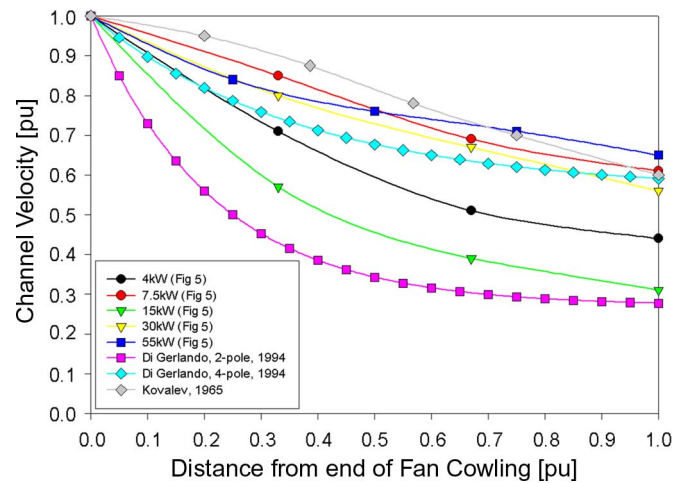


Fig. 6. Fin channel air velocity versus the distance from fan (the base speed is the inlet air velocity in the fin channels).

the shaft speed is a linear relationship. The actual velocity from channel to channel can vary significantly and is a function of the fan direction. In fact, in many TEFC machines, some of the fin channels on the machine frame may be blocked by bolt lugs and terminal boxes [19].

Alternatively, it is possible to consider the volume flow rate. If the channel dimensions and the inner cowling diameter are known, the inlet velocity can be calculated on the base of the cross-sectional area available for flow.

A factor that must be taken account of in a TEFC machine is that air tends to leak out of the open channels. Consequently, the local air velocity at the drive end is lower than that at the non-drive end (fan side).

The typical form of the reduction in velocity versus the distance from the fan is shown in Fig. 6. The prediction of the actual reduction in velocity is a complex function of many factors, including the fan type, the fin and cowling design, and the rotational speed. Using experimental data and/or CFD results, it is possible to define a more accurate model for the finned housing [9], [20]. For machines similar to the TEFC induction motors shown in Fig. 3, the relationships shown in Figs. 5 and 6 can be used to obtain a reasonable starting value of the air velocity along the fin channels.

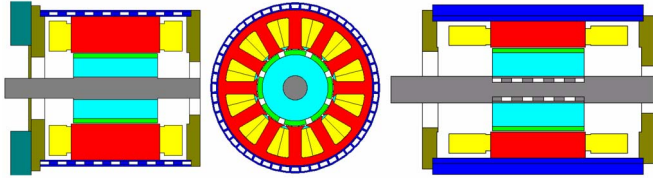


Fig. 7. Examples of liquid cooling system types.

## V. FORCED CONVECTION: WATER JACKETS

Liquid cooling methods such as spiral grooves and zigzag arrangements of axial covered channels are often used in highly loaded machines. Fig. 7 shows examples of typical liquid cooling duct systems. Correlations that are suitable for internal flow are used to calculate the heat transfer coefficient in such cases. The heating effect of the fluid is also taken into account in the formulation.

### A. Laminar Flow

Depending on the channel shapes, different correlations have to be used [7]. In particular, (15) is for round channels, (16) is for rectangular channels, and (17) is for concentric cylinders. We have

$$\text{Nu} = 3.66 + \frac{0.065 \cdot (D/L) \cdot \text{Re} \cdot \text{Pr}}{1 + 0.04 \cdot ((D/L) \cdot \text{Re} \cdot \text{Pr})^{2/3}} \quad (15)$$

$$\text{Nu} = 7.49 - 17.02 \cdot \frac{H}{W} + 22.43 \cdot \left(\frac{H}{W}\right)^2 - 9.94 \cdot \left(\frac{H}{W}\right)^3 + \frac{0.065 \cdot (D/L) \cdot \text{Re} \cdot \text{Pr}}{1 + 0.04 \cdot ((D/L) \cdot \text{Re} \cdot \text{Pr})^{2/3}} \quad (16)$$

$$\text{Nu} = 7.54 + \frac{0.03 \cdot (D/L) \cdot \text{Re} \cdot \text{Pr}}{1 + 0.016 \cdot ((D/L) \cdot \text{Re} \cdot \text{Pr})^{2/3}} \quad (17)$$

where the  $H/W$  ratio is the channel height-to-width ratio, and  $D$  is the channel hydraulic diameter, which is two times the gap for concentric cylinders and four times the channel cross-sectional area divided by the channel perimeter for round and rectangular channels. The variable part of the above equation is the entrance length correction, which accounts for entrance lengths where the velocity and temperature profiles are not fully developed [21].

### B. Turbulent Flow

For fully developed turbulent flow (i.e.,  $3000 < \text{Re} < 10^6$ ), the following correlation is available [22]:

$$\text{Nu} = \frac{f}{8} \cdot \frac{(\text{Re} - 1000) \cdot \text{Pr}}{1 + 12.7 \cdot (f/8)^{0.5} \cdot (\text{Pr}^{2/3} - 1)} \quad (18)$$

where  $f$  is the friction factor, and for a smooth wall, it can be estimated by

$$f = [0.790 \cdot \ln(\text{Re}) - 1.64]^{-2}. \quad (19)$$

The flow is assumed to be fully laminar when  $\text{Re} < 2300$  in round and rectangular channels and when  $\text{Re} < 2800$  in concentric cylinders. The flow is assumed to be fully turbulent

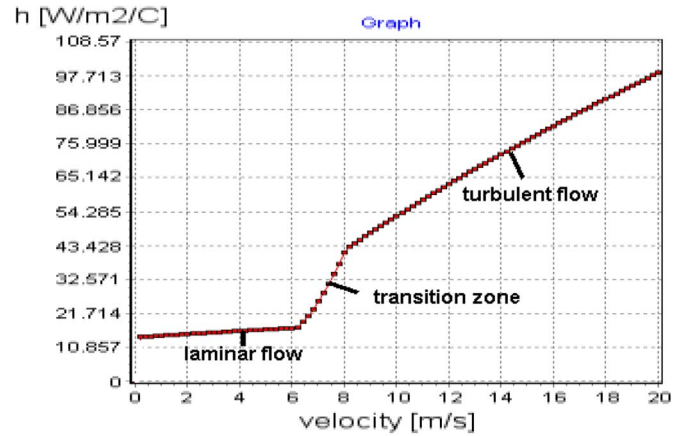


Fig. 8. Enclosed channel forced convection heat transfer coefficient versus the fluid velocity.

when  $\text{Re} > 3000$ , even if, in practice, the flow may not be fully turbulent until  $\text{Re} > 10000$ . The transition between laminar and turbulent flow is assumed for  $\text{Re}$  values between those given above. Typical results showing transition from a laminar to a turbulent flow are shown in Fig. 8 for the enclosed channel correlation. Fig. 8 highlights that the two formulations do not join each other and a small transition zone (starting from the critical  $\text{Re}$  number, which is dependent upon the channel shape up to 3000) is used to make the two functions join and to obtain numerical stability. A weighted average (based on  $\text{Re}$ ) is then used to calculate  $\text{Nu}$  in the transition zone.

## VI. FORCED CONVECTION: END-SPACE REGIONS

Convection for all surfaces within the internal sections of the machine must be modeled; this is particularly important for the end-windings since they are typically the hottest point in the machine. The convection cooling of internal surfaces can be complex because the fluid flow depends on many factors, including the end-winding shape and length, added fanning effects due to wafers (i.e., simple fan features that are included on induction motor squirrel-cage end-rings), simple internal fans, surface finish of the rotor end sections, and turbulence. Several authors have studied such a cooling phenomenon, and in general, they propose the following equation as a useful formulation [9]:

$$h = k_1 \cdot [1 + k_2 \cdot v^{k_3}] \quad (20)$$

where  $k_1$ ,  $k_2$ , and  $k_3$  are curve fit coefficients, and  $v$  is the average air velocity for the surface under consideration. There are several surfaces within the end-space (i.e., end winding inner and outer surfaces, endcap inner surface, housing inner surface, shaft surface, etc.), all with different average air velocities. For example, the outer surface of the endwinding will have a much lower velocity, compared to the inner surface, as it is shielded from the air movement within the endcaps, which is induced by rotational fanning effects. It is usual to try to estimate each surface average air velocity based on the maximum rotor peripheral velocity, the size of any internal fans, and the amount by which a surface is shielded from the main rotational airflow.

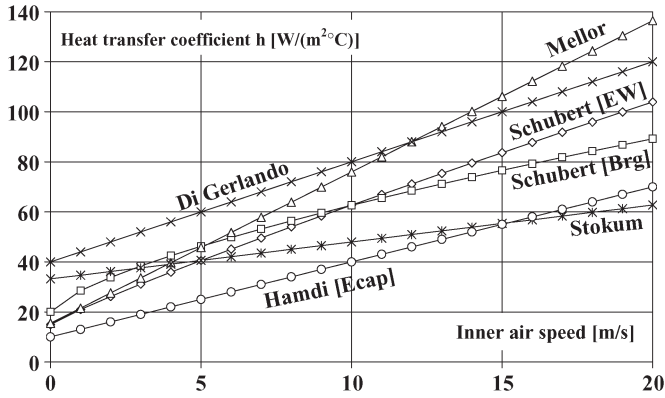


Fig. 9. End-space convection heat transfer coefficients versus the inner air velocity.

Fig. 9 shows some published correlations related to the end-space cooling. It is interesting that all the references show much the same trends. A detailed discussion about these topics can be found in [23].

VII. FORCED CONVECTION: AIR-GAP HEAT TRANSFER

The traditional method to account for heat transfer across the electrical machine air gaps is to use the dimensionless convection correlations developed from testing on smooth concentric rotating cylinders by Taylor [24].

In order to judge if the flow in the air gap is laminar, vortex, or turbulent, the Taylor number ( $Ta$ ) has to be calculated using

$$Ta = Re \cdot (l_g/R_r)^{0.5} \tag{21}$$

where  $l_g$  is the air-gap radial thickness,  $R_r$  is the rotor outer radius, and  $Re = l_g \cdot v/\mu$ .

The flow is laminar if  $Ta < 41$ . In this case,  $Nu = 2$ , and heat transfer is by conduction only. If  $41 < Ta < 100$ , the flow takes on a vortex form with enhanced heat transfer; in this case, the following equation has to be used:

$$Nu = 0.202 \cdot Ta^{0.63} \cdot Pr^{0.27} \tag{22}$$

If  $Ta > 100$ , the flow becomes fully turbulent, and a further increase in heat transfer results. In this condition, the following equation is used to calculate  $Nu$ :

$$Nu = 0.386 \cdot Ta^{0.5} \cdot Pr^{0.27} \tag{23}$$

Gazley [10] investigated the effect of both rotor and stator slotting on the air-gap heat transfer. He found that slotting gave a relatively minor change in air-gap heat transfer in most cases. There was a small decrease in heat transfer for the laminar flow and a small increase in heat transfer for the vortex flow. He found that there could be a significant increase in heat transfer due to slotting with highly turbulent flow, but equations were not given to quantify the effect.

VIII. FORCED CONVECTION: THROUGH VENTILATION

In the through-ventilation model, the airflow through the machine can be calculated using flow network analysis [11]–[14].

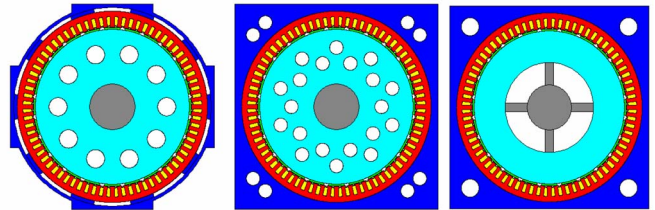


Fig. 10. Examples of typical inner ventilation duct types.

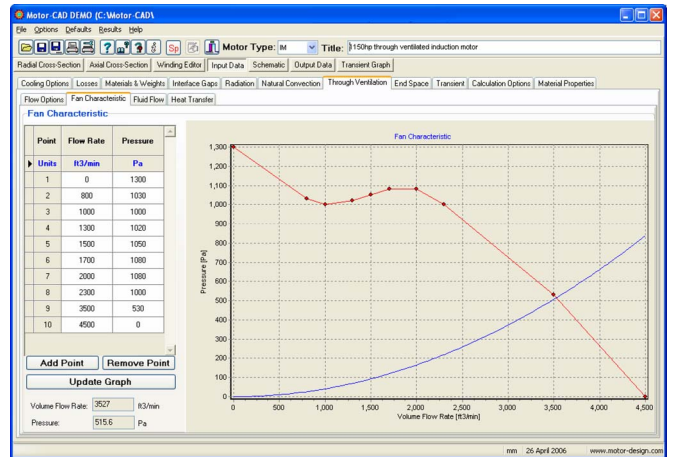


Fig. 11. Fan and system resistance characteristics screenshot in [3].

Typically, there are three parallel flow paths inside the machine: 1) stator ducts; 2) rotor ducts; and 3) the air gap. Examples of typical duct types are shown in Fig. 10. The total flow through the machine is determined from the intersection of the fan characteristic and the system flow resistance characteristic, as shown in Fig. 11 [3]. The flow velocity in each section of the flow circuit is calculated from the local flow rate and the local cross-sectional area. The velocity information is then used to calculate the local heat transfer coefficients and, subsequently, the thermal resistances.

IX. FLOW NETWORK ANALYSIS

The governing equation that relates pressure drop  $P$  (flow equivalent of electrical voltage, in pascals) to volume flow rate  $Q$  (equivalent to electrical current,  $[m^3/s]$ ) and flow resistance  $R$   $[kg/m^7]$  is

$$P = R \cdot Q^2. \tag{24}$$

It is important to highlight that in (24), the formulation is in terms of  $Q^2$  rather than  $Q$  due to the turbulent nature of the flow. Two types of flow resistance exist: 1) where there is a change in flow condition, such as expansions and contractions and bends, and 2) due to the fluid friction at the duct wall surface; in electrical machines, this is usually negligible compared to the first resistance type due to the comparatively short flow paths. The flow resistance is calculated for all changes in the flow path using

$$R = \frac{k \cdot \rho}{2 \cdot A^2}. \tag{25}$$

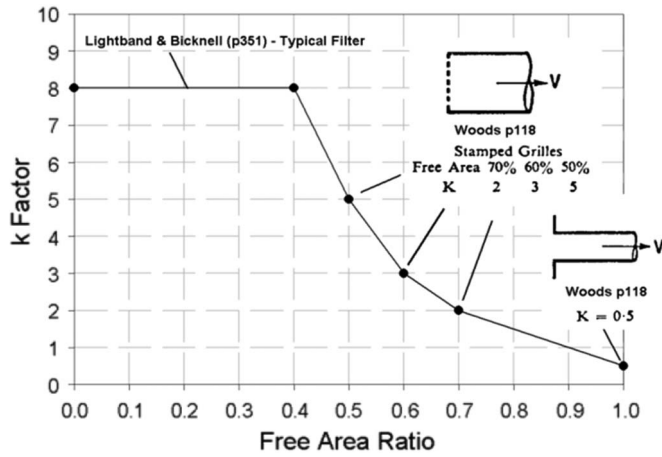


Fig. 12. Inlet grill  $k$  factor.

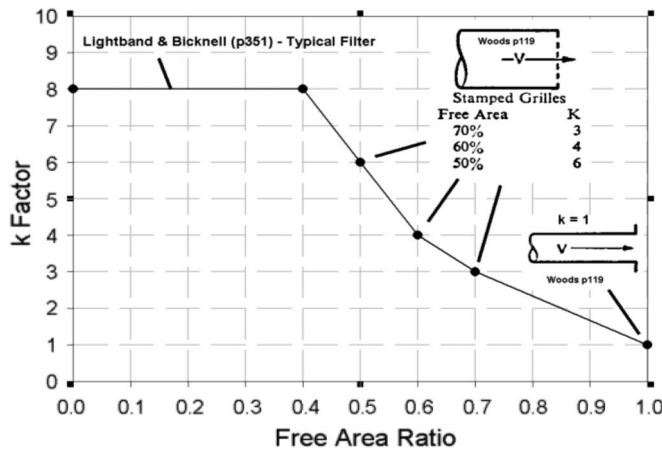


Fig. 13. Outlet grill  $k$  factor.

In (25),  $k$  is the dimensionless coefficient of local fluid resistance (sometimes called minor loss factor),  $\rho$  (in kilograms per cubic meter) is the air density, and  $A$  (in square meters) is the area of the flow section that is defined in the minor loss factor formulation. The value of  $k$  depends upon the local flow condition, i.e., if there is an obstruction, expansion, contraction, etc. Suitable formulations are available to calculate the  $k$  factors for all changes in the flow section within the motor. A feature of the thermal tool [3] is that it automatically selects the most appropriate formulation for all the flow path components in the through-ventilation scheme selected, i.e., a sudden contraction when air enters the stator/rotor ducts, a 90° bend where the air passes around the end winding, etc.

Five types of flow resistance are used to model the flow through the machine:

- 1) inlet grill/guard;
- 2) outlet grill/guard;
- 3) sharp bend;
- 4) sudden expansion;
- 5) sudden contraction.

A. Inlet and Outlet Grill/Guards

The characteristic shown in Fig. 12 is used to calculate pressure drop at entry to system due to a grill/filter over the inlet

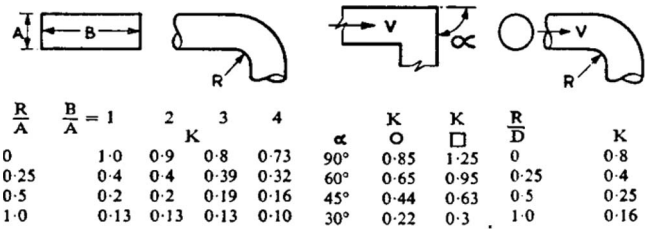


Fig. 14.  $k$  factor values for bends.

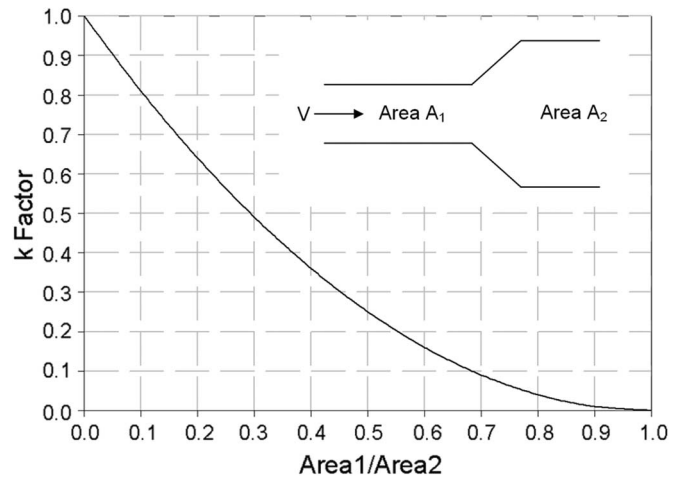


Fig. 15. Sudden expansion  $k$  factor.

vents. A similar characteristic is used for outlet vents as well, as shown in Fig. 13. Both use a data combination from Woods of Colchester Ltd., [12] and Lightband and Bicknell [13]. The arrows in these pictures relate to which area is used in the flow resistance calculation.

B. Sharp Bend

The worst case of a right angle bend is assumed in the flow calculation ( $k = 1$ ). It is possible to use the average area at each end of the bend. Fig. 14 shows  $k$  data for other types of bend [12].

C. Sudden Expansions and Contractions

The  $k$  factor for a sudden expansion can be calculated using (26) [12], [13]. A plot of the formulation is shown in Fig. 15. We have

$$k = (1 - \text{Area}_1/\text{Area}_2)^2. \tag{26}$$

The  $k$  factor for a sudden contraction is shown in Fig. 16. Note that the arrows shown in Figs. 15 and 16 indicate which area should be used in (25). Modified  $k$  factors are also available for graded expansions and contractions [11]–[13].

The  $k$  factor for the rotor duct entry contraction can be adjusted for rotation effects using [14]

$$k_{\text{rot}} = k_{\text{static}} \cdot \frac{V_{\text{rot}}^2 + V_{\text{air}}^2}{V_{\text{air}}^2} \tag{27}$$

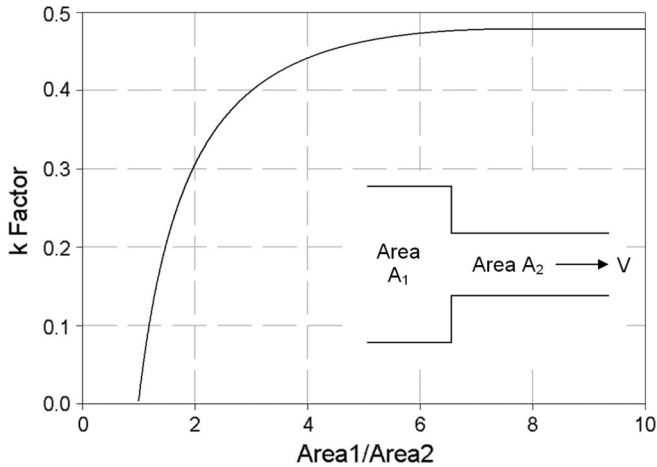


Fig. 16. Sudden contraction  $k$  factor.

where

- $k_{rot}$  minor loss factor with rotation;
- $k_{static}$  minor loss factor with no rotation;
- $V_{rot}$  average peripheral velocity of rotor ducts;
- $V_{air}$  axial velocity of air through the ducts.

This takes into account the increase in the pressure drop due to the rotational speed in rotating ducts. This adjustment is applied to all ducts on the rotor. It is more questionable if such an adjustment should also be applied to the air gap and the user is free to make a choice.

X. CONCLUSION

In this paper, a comprehensive set of convection heat transfer and flow resistance formulations that are suitable for thermal analysis of electric machines has been presented. Most of the formulations are empirical based and in terms of dimensionless numbers. This gives benefits in terms of maximum reuse of the relationships developed, i.e., the same formulation can be used for similarly shaped geometries with a size that is different from that of the original experiments and/or with a different fluid. This paper can be considered as a reference that brings together useful formulations for calculating convection and flow in electrical machines.

REFERENCES

[1] Z. Gao, T. G. Habetler, R. G. Harley, and R. S. Colby, "A sensorless rotor temperature estimator for induction machines based on a current harmonic spectral estimation scheme," *IEEE Trans. Ind. Electron.*, vol. 55, no. 1, pp. 407–416, Jan. 2008.

[2] J. J. Nelson, G. Venkataramanan, and A. M. El-Refaie, "Fast thermal profiling of power semiconductor devices using Fourier techniques," *IEEE Trans. Ind. Electron.*, vol. 53, no. 2, pp. 521–529, Apr. 2006.

[3] *Motor-CAD*. [Online]. Available: www.motor-design.com

[4] A. Boglietti, A. Cavagnino, M. Parvis, and A. Vallan, "Evaluation of radiation thermal resistances in industrial motors," *IEEE Trans. Ind. Appl.*, vol. 42, no. 3, pp. 688–693, May/June. 2006.

[5] F. P. Incropera and D. P. DeWitt, *Introduction to Heat Transfer*. Hoboken, NJ: Wiley, 1990.

[6] J. P. Holman, *Heat Transfer*. New York: McGraw-Hill, 1997.

[7] A. F. Mills, *Heat Transfer*. Englewood Cliffs, NJ: Prentice-Hall, 1999.

[8] W. S. Janna, *Engineering Heat Transfer*. London, U.K.: Van Nostrand Reinhold (International), 1988.

[9] D. Staton, A. Boglietti, and A. Cavagnino, "Solving the more difficult aspects of electric motor thermal analysis, in small and medium size industrial induction motors," *IEEE Trans. Energy Convers.*, vol. 20, no. 3, pp. 620–628, Sep. 2005.

[10] C. Gazley, "Heat transfer characteristics of rotating and axial flow between concentric cylinders," *Trans. ASME*, pp. 79–89, Jan. 1958.

[11] I. E. Idel'chik, *Handbook of Hydraulic Resistance—Coefficients of Local Resistance and of Friction*. Washington, DC: Nat. Sci. Found., 1960.

[12] *Woods Practical Guide to Fan Engineering*, Woods Colchester Ltd., Colchester, U.K., Jun. 1960.

[13] D. A. Lightband and D. A. Bicknell, *The Direct Current Traction Motor: Its Design and Characteristics*. London, U.K.: Business Books Ltd., 1970.

[14] J. L. Taylor, *Calculating Air Flow Through Electrical Machines*. Kent, U.K.: Electrical Times, Jul. 21, 1960.

[15] F. Heiles, "Design and arrangement of cooling fins," *Elektrotechnik und Maschinenbau*, vol. 69, no. 14, pp. 42–48, Jul. 1952.

[16] D. W. Van De Pol and J. K. Tierney, "Free convection Nusselt number for vertical U-shaped channels," *Trans. ASME*, vol. 95, pp. 542–543, Nov. 1973.

[17] C. D. Jones and L. F. Smith, "Optimum arrangement of rectangular fins on horizontal surfaces for free-convection heat transfer," *Trans. ASME*, vol. 92, pp. 6–10, Feb. 1970.

[18] D. A. Staton and E. So, "Determination of optimal thermal parameters for brushless permanent magnet motor design," in *Conf. Rec. IEEE IAS Annu. Meeting*, St. Louis, MO, Oct. 1998, pp. 41–49.

[19] A. Boglietti, A. Cavagnino, and D. Staton, "Determination of critical parameters in electrical machine thermal models," in *Conf. Rec. IEEE IAS Annu. Meeting*, Sep. 2007, pp. 73–80.

[20] M. A. Valenzuela and J. A. Tapia, "Heat transfer and thermal design of finned frames for TEFC variable speed motors," in *Proc. Conf. Rec. IEEE IECON*, Paris, France, Nov. 6–10, 2006, pp. 4835–4840. CD-ROM.

[21] D. K. Edwards, V. E. Denny, and A. F. Mills, *Transfer Processes*, 2nd ed. Washington, DC: Hemisphere, 1979.

[22] V. Gnielinski, "New equations for heat and mass transfer in turbulent pipe and channel flow," *Int. Chem. Eng.*, vol. 16, pp. 359–368, 1976.

[23] A. Boglietti and A. Cavagnino, "Analysis of endwinding cooling effects in TEFC induction motors," *IEEE Trans. Ind. Appl.*, vol. 43, no. 5, pp. 1214–1222, Sep./Oct. 2007.

[24] G. I. Taylor, "Distribution of velocity and temperature between concentric cylinders," *Proc. Roy Soc.*, vol. 159, pt. A, pp. 546–578, 1935.



**David A. Staton** received the Ph.D. degree in CAD of electrical machines from Sheffield University, Sheffield, U.K., in 1985.

He has worked on motor design, particularly the development of motor design software, with Thorn EMI, the SPEED Laboratory at Glasgow University, Glasgow, U.K., and Control Techniques. In 1999, he set up a new company, Motor Design Ltd., Shropshire, U.K., to develop thermal analysis software for electrical machines.



**Andrea Cavagnino (M'05)** was born in Asti, Italy, in 1970. He received the M.Sc. and the Ph.D. degrees in electrical engineering from the Politecnico di Torino, Torino, Italy, in 1995 and 1999, respectively.

Since 1997, he has been with the Electrical Machines Laboratory, Department of Electric Engineering, Politecnico di Torino, where he is currently an Assistant Professor. His fields of interest include electromagnetic design, thermal design, and energetic behaviors of electric machines. He has authored more than 60 papers published in technical journals

and conference proceedings.

Dr. Cavagnino is a Registered Professional Engineer in Italy. Since 2007, he has been an Associate Editor for the Electrical Machine Committee-IEEE TRANSACTIONS ON INDUSTRIAL APPLICATIONS.